Fabrication of GaN-based Photonic Crystal Structures by Reactive Ion Etching

Junjun Wang

The fabrication of the 2D GaN-based photonic crystal structure at optical scales, a sub-μm scale in our case is very challenging. In our work, a double-etching method proved to be feasible to achieve the periodic GaN/air variation. The pattern was defined in a PMMA resist by electron-beam lithography and transferred to SiO_2 by reactive ion etching (RIE) in a CF_4 plasma and further into GaN by RIE in a chlorine plasma. An interesting phenomenon during RIE was observed: the etching rate at the barrier site is enhanced to about two times of that in the μm scale while the etching rate at the valley site stays the same. If the mask is exhausted during RIE, the etching depth increases before the mask disappearance and decreases after that with further etching. Thus the etching time is a critical parameter to obtain deep enough holes in GaN. Referring to the etching rates of Si_3N_4 and SiO_2 in both kinds of plasma, it might be easier to achieve deep holes when Si_3N_4 substitutes SiO_2.

1. Introduction

Photonic crystals (PC) are structures with periodic variations of the refractive index. In such structures, the light propagation can be controlled or manipulated in a similar way as the electronic energetic bands in crystals by defining photonic bands. Since the first realization of a non-one-dimensional PC in 1987 [1], the PC has attracted much interest worldwide. GaN-based two-dimensional (2D) photonic crystal surface-emitting lasers (PCSEL) are promising to produce single mode lasing over a large area in high power blue-violet emitter applications [2–4]. However, it is challenging to fabricate such a GaN-based PC at an optical wavelength scale. There are very few publications about this topic up to now.

The PC fabrication methods can be considered as either "Bottom Up" or "Top Down" approaches. In the former, periodic GaN pyramids are formed by selective area growth on hexagonally-patterned templates in metal-organic vapor phase deposition system [5]. The refractive index changes gradually at the GaN/air edge in such a pyramidal structure and does not have a high contrast. In this report, a "Top Down" method will be described: the pattern was defined in PMMA by electron beam lithography (EBL) and transferred step by step into GaN by reactive ion etching (RIE). The experimental details will be described in the following.

Our final goal is to integrate the PC into a GaN-based laser diode (LD) emitting at around 410 nm. Based on the calculation of the photonic band diagram, a square lattice

is designed with a hole radius between 60 and 80 nm and the lattice constant between 330 and 380 nm. In order to make the emission interfere better with the PC, the holes should be deep enough to penetrate the waveguide or even the InGaN/GaN quantum wells. So our initial goal is to reach $\sim$ 400 nm deep homogeneous holes in the GaN-based LD.

The main feature of our structure is its sub-μm-scaled size which requires the employment of EBL to define the lattice pattern instead of standard photolithography and determines its special behavior during RIE when the PC pattern is transferred from the EBL resist into the semiconductor structure.

2. Fabrication Processes

The processing steps were investigated using test samples that simply contain 5 pairs InGaN/GaN quantum wells grown on c-plane GaN rather than the LD. The following two kinds of fabrication processes were tried: the single-step and double-step etching methods. The infeasibility of the first one motivate us to investigate the second: to transfer the PC pattern into the sample by CF_4 RIE and chlorine RIE step by step.

2.1 Single-step etching method

Sample A was firstly covered with a layer of the EBL resist of PMMA by spin coating. By EBL we defined the square pattern in the PMMA layer. The whole PC pattern is defined in a square shape with a size of $750\times750\,\mu m^2$. Then, with PMMA acting as mask, the sample was etched by RIE in a chlorine plasma (details shown in Table 1) for 5 min to transfer the PC pattern into the sample. Finally we intended to remove PMMA with 1-methyl-2-pyrrolidone (MP). The PMMA within the circular ring around holes still exists

Table 1: RIE parameters in a chlorine plasma.

Electrode RF power	100 W
Pressure	2 Pa
Cl_2	1.5 sccm
BCl_3	10 sccm
Ar	10 sccm

after we tried to remove it with $\sim$120 °C MP solution. Part of the PMMA rings were removed mechanically by tweezers unintentionally as the gray stripes in Fig. 1. Actually the PMMA was polymerized during the chlorine RIE and became quite resistant. So the single-step etching method proved to be infeasible.

2.2 Double-step etching method

In order to overcome this problem, we developed a double-step etching method employing two masks PMMA and SiO_2 with the later under the former: A layer of 700 nm SiO_2 was

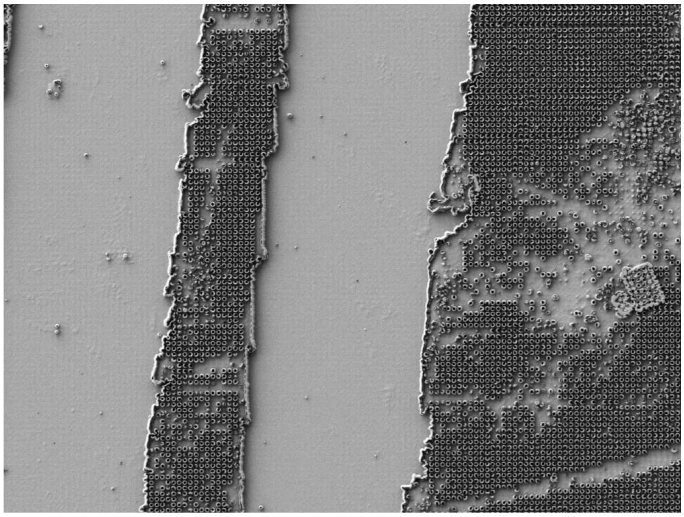

Fig. 1: Top view of sample A.

Table 2: RIE parameters in a CF_4 plasma.

Electrode RF power	60 W
Pressure	5.3 Pa
CF_4	45 sccm

deposited on the samples by plasma-enhanced chemical vapor deposition, followed by a PMMA layer of ∼620 nm. The same PC pattern was defined in PMMA by EBL as that in the single-step etching method. Subsequently, the PC pattern was transferred to the SiO_2 film by RIE in a CF_4 plasma (details shown in Table 2) which did not polymerize the PMMA layer. After removing PMMA with hot MP, the sample was etched by RIE using chlorine plasma with the structured SiO_2 layer as mask. In order to gain a better understanding how both of these etching processes behave, two samples were prepared: sample B before and sample C with the GaN etching in chlorine plasma. The etching times for these two samples are shown in Table 3.

Table 3: The etching periods for sample B and C.

	CF_4 RIE	Chlorine RIE
Sample B	10 min40 sec	—
Sample C	10 min20 sec	10 min

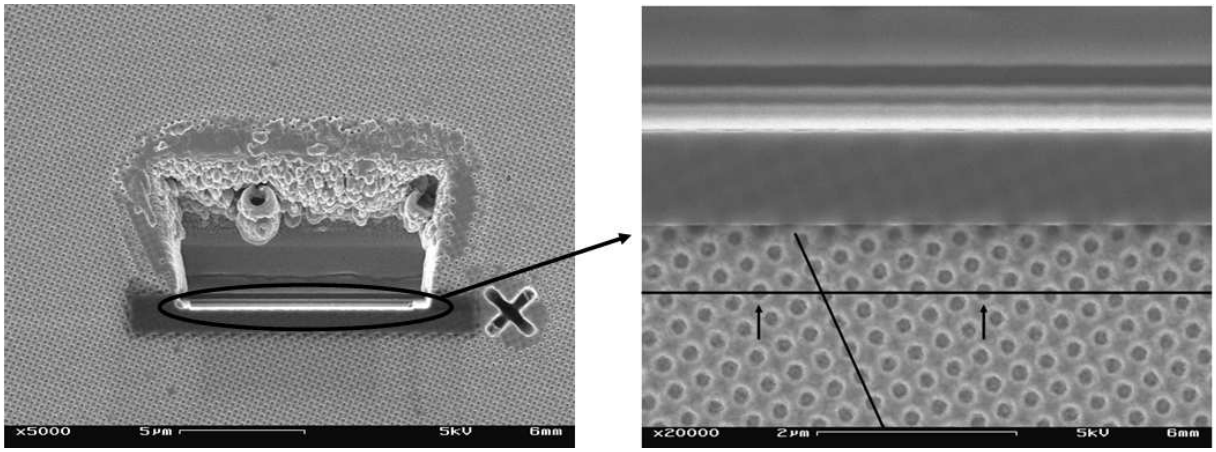

Fig. 2: The groove cut by FIB (left) and the magnified lower side of the groove (right).

3. Focused Ion Beam Characterization

A cross-section image of the PC structure is necessary to evaluate the hole depth and profile. As mentioned, the whole PC pattern is defined in a square shape with a size of $750\times750\,\mu m^2$. Therefore, it is very difficult to cleave exactly through such a small area manually or even with a cleaving saw. In such a case, focused ion beam (FIB) turns to be a good choice to characterize the PC cross section. The FIB setup resembles a scanning electron microscope (SEM). While the SEM uses a focused beam of electrons to image the sample, the FIB uses a focused beam of ions instead to image or manipulate the sample. FIB is a destructive method and can be applied to cut a local groove of a few μm^2 (as shown in Fig. 2) into the sample. Then it is possible to characterize the PC cross section from the groove sidewall.

Before the samples were put into the FIB chamber, 80 nm Ni was deposited over the whole sample surface for a better contrast. A layer of C was deposited in the FIB chamber only within several tens μm^2 (the black region in Fig. 2) to avoid the GaN redeposition during milling of the groove.

The images of the PC cross section were taken with such an orientation that the bird's eye views of both the sample surface and groove sidewall are visible in the image (Fig. 3 (left) as an example). Additionally the software integrated in the FIB setup adjusted the lower part of the image for the groove sidewall part to appear in an exact cross section view.

4. Results and Discussion

FIB was utilized to characterize the hole cross section of sample B and C. The depth and the shape of the holes are of our interest. The holes get narrower near the bottom. So it is necessary for FIB to cut exactly through the hole center in order to gain the depth and the diameter of the holes. If the cut is parallel to the photonic crystal direction $\langle 01\rangle$, it is impossible to handle FIB so accurately that the cut is placed at the hole centers in one

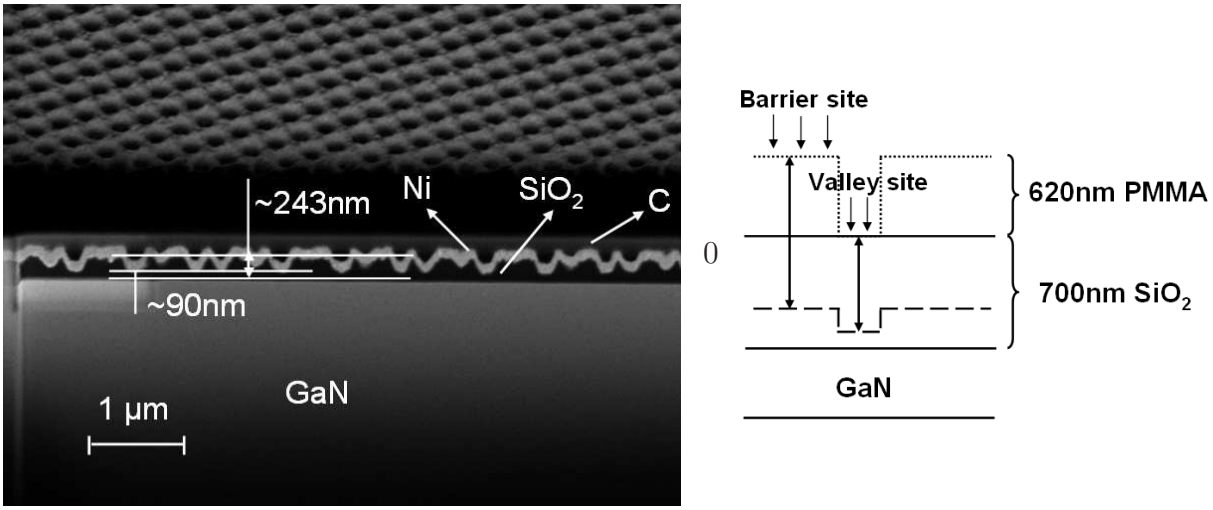

Fig. 3: The FIB image (left) and the schematic diagram about the surface development during the CF_4 RIE (right) of sample B.

line. The trick is to rotate the cut with a certain angle from the ⟨01⟩ direction and the cut crosses holes with many different distances away from the centers. Some of them are close enough to 0 indicated by arrows in Fig. 2 (right) which correspond to the deepest holes in Fig. 3 (left).

The sub-µm-scaled size of the PC structure causes a quite different RIE behavior compared to a micrometer-scaled structure. The specific RIE behavior will be discussed in the following.

For sample B, the PMMA was totally etched away and the SiO_2 was reduced to ∼243 nm with ∼153 nm deep holes in it during the CF_4 RIE. The etching process is schematically shown in Fig. 3 (right): 610 nm SiO_2 at the valley site and 620 nm PMMA + 457 nm SiO_2 at the barrier site were etched away. Then the etching rate at the valley site can be calculated to be 57 nm/min which corresponds very well to the estimation of ∼60 nm/min from the µm-scaled samples. The SiO_2 and PMMA etching rates in our RIE setup were evaluated to be ∼60 nm/min and 40 nm/min on µm-scaled samples. The ratio of 57:40 between the etching rates of SiO_2 and PMMA under the same RIE condition tells us that 884 nm SiO_2 needs the same time to be etched away as 620 nm PMMA. So 620 nm PMMA + 457 nm SiO_2 could be substituted by 1341 nm SiO_2 with respect to the etching rate. Hence, an effective etching rate of 125 nm/min is calculated for SiO_2 at the barrier site. Obviously, the same etching rate at the valley site and a doubled etching rate at the barrier site occur in the sub-µm-scaled structure compared to the µm-scaled one.

For sample C, the image of the cross section is shown in Fig. 4 (left): SiO_2 was totally etched away leaving 92 nm deep holes in GaN. The etching process is schematically shown in Fig. 4 (right). Here, etching rates of SiO_2 and GaN under the chlorine plasma RIE condition (Table 1) in our etching system are evaluated to be 16.6 nm/min and 45 nm/min, respectively. Assuming the etching rate ratio between the barrier and the valley sites to be λ, two equations describing the chlorine plasma etching are like the following:

$$\frac{243}{16.6\lambda} + \frac{x}{45\lambda} = 10 \tag{1}$$

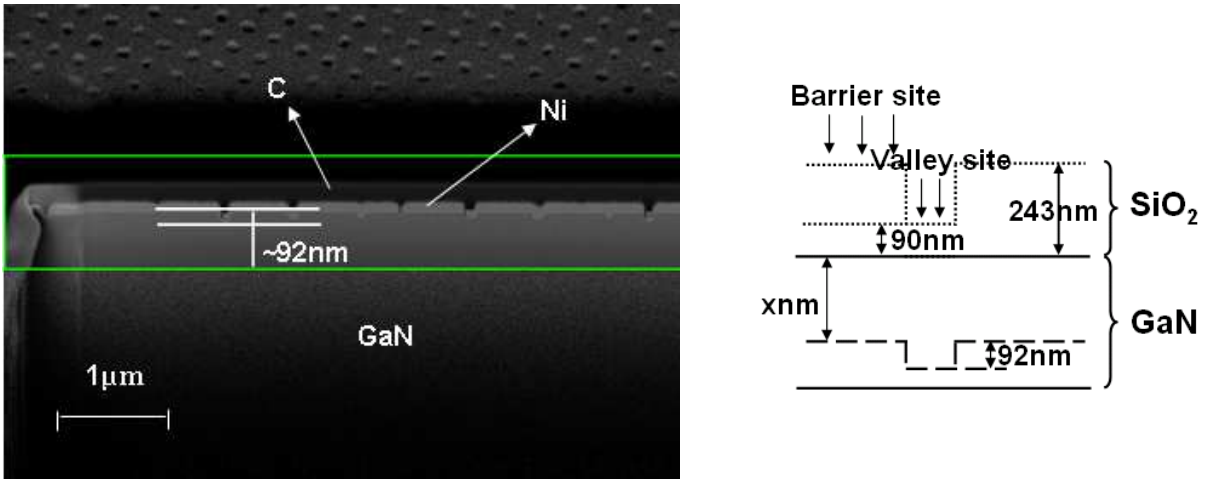

Fig. 4: The FIB image (left) and the schematic diagram about the surface development during the CF_4 RIE (right) of sample C.

$$\frac{90}{16.6} + \frac{x+92}{45} = 10 \tag{2}$$

λ is calculated to be 2.1 which is close to the value in CF_4 plasma etching.

Not only physical sputtering but also chemical erosion are involved in RIE. The former part is an anisotropic element while the latter is an isotropic one. The chemical erosion attacks the barrier from both the surface and the sidewall, but only has the chance to attack the valley vertically. So the etching rate at the barrier is enhanced compared to the valley site. Additionally, our PC structure (the sub-µm scale) has a high surface-to-volume ratio. This leads to an even larger etching rate enhancement at the barrier site which explains the above mentioned observation.

It is clear that the hole depth decreases when the etching rate at the barrier site is larger than that at the valley site. So after the mask is etched away completely, the hole depth reduces and the PC structure is smeared with further etching. The hole depth reaches its maximum at the point when the mask is etched away.

In order to transfer a deeper pattern from PMMA into the 2nd mask (SiO_2 in the above experiments), either the PMMA thickness or the PMMA/2nd mask selectivity in CF_4 RIE should be increased. However, the PMMA thickness is limited by the EBL resolution. Therefore, a high etching rate of the 2nd mask in CF_4 RIE is required. On the other hand, a low etching rate of the 2nd mask in chlorine RIE enables a longer etching time to transfer a deeper PC pattern into GaN. Referring to Table 4 Si_3N_4 has a pronounced advantage in CF_4 RIE with a relatively small disadvantage in chlorine RIE compared to SiO_2. In this sense, Si_3N_4 is a better candidate than SiO_2 as the 2nd mask.

Taking the above discussion into account, new samples have been designed and prepared. Currenly the FIB characterization is ongoing.

Table 4: The etching rates of SiO_2 and Si_3N_4 under different RIE conditions.

etching rate (nm/min)	CF_4 RIE	chlorine RIE
SiO_2	60	16.6
Si_3N_4	180	22

5. Conclusion and Outlook

A fabrication method for a photonic crystal structure in GaN-based materials was investigated to create a periodic 2D pattern of air holes. A single-etching method was proved to be infeasible. A double-step etching method was implemented resulting in successful etching of periodic air holes in GaN. An interesting phenomenon for reactive ion etching of the sub-μm-scaled PC structure was found: $\sim$ doubled etching rate at the barrier site compared to the valley site. This indicates us the etching time is a critical parameter to obtain deep enough patterns. Si_3N_4 could be a good candidate acting as the 2nd mask. A three-layer resist system PMMA/Ti/AZ1350J is also promising to define the square pattern into GaN in the sub-μm scale [6].

6. Acknowledgments

Much valuable technical support was given by Ilona Argut, Yakiv Mens, Lorenz Lechner and Rudolf Rösch. Many fruitful discussions were done with Robert Leute and Mohamed Fikry.

References

[1] E. Yablonovitch, "Inhibited Spontaneous Emission in Solid-State Physics and Electronics", *Phys. Rev. Lett.*, vol. 58, pp. 2059–2062, 1987.

[2] T.C. Lu, S.W. Chen, L.F. Lin, T.T. Kao, C.C. Kao, P. Yu, H.C. Kuo, S.C. Wang, and S. Fan, "GaN-based two-dimensional surface-emitting photonic crystal lasers with AlN/GaN distributed Bragg reflector", *Appl. Phys. Lett.*, vol. 92, pp. 011129-1–3, 2008.

[3] S.W. Chen, T.C. Lu, Y.J. Hou, T.C. Liu, H.C. Kuo, and S.C. Wang, "Lasing characteristics at different band edges in GaN photonic crystal surface emitting lasers", *Appl. Phys. Lett.*, vol. 96, pp. 071108-1–3, 2010.

[4] T.C. Lu, S.W. Chen, T.T. Kao, and T.W. Liu, "Characteristics of GaN-based photonic crystal surface emitting lasers", *Appl. Phys. Lett.*, vol. 93, pp. 111111-1–3, 2008.

[5] T. Wunderer, J. Wang, F. Lipski, S. Schwaiger, A. Chuvilin, U. Kaiser, S. Metzner, F. Bertram, J. Christen, S.S. Shirokov, A.E. Yunovich, and F. Scholz, "Semipolar

GaInN/GaN light-emitting diodes grown on honeycomb patterned substrates", *phys. stat. sol. (c)*, vol. 7, pp. 2140–2143, 2010.

[6] E. Bassous, L.M. Ephrath, G. Pepper, and D.J. Mikalsen, "A Three-Layer Resist System for Deep U.V. and RIE Microlithography on Nonplanar Surfaces", *J. Electrochem. Soc.*, vol. 130, pp. 478–484, 1983.